Effective tight-binding models for excitons in branched conjugated molecules

Hao Li,[1] Sergey V. Malinin,[2] Sergei Tretiak,[1,3,a)] and Vladimir Y. Chernyak[2,b)]
[1]*Theoretical Division and Center for Nonlinear Studies, Los Alamos National Laboratory, Los Alamos, New Mexico 87545, USA*
[2]*Department of Chemistry, Wayne State University, 5101 Cass Avenue, Detroit, Michigan 48202, USA*
[3]*Center for Integrated Nanotechnologies, Los Alamos National Laboratory, Los Alamos, New Mexico 87545, USA*

(Received 2 May 2013; accepted 29 July 2013; published online 14 August 2013)

Effective tight-binding models have been introduced to describe vertical electronic excitations in branched conjugated molecules. The excited-state electronic structure is characterized by quantum particles (excitons) that reside on an irregular lattice (graph) that reflects the molecular structure. The methodology allows for the exciton spectra and energy-dependent exciton scattering matrices to be described in terms of a small number of lattice parameters which can be obtained from quantum-chemical computations using the exciton scattering approach as a tool. We illustrate the tight-binding model approach using the time-dependent Hartree-Fock computations in phenylacetylene oligomers. The on-site energies and hopping constants have been identified from the exciton dispersion and scattering matrices. In particular, resonant, as well as bound states, are reproduced for a symmetric quadruple branching center. The capability of the tight-binding model approach to describe the exciton-phonon coupling and energetic disorder in large branched conjugated molecules is briefly discussed. © *2013 AIP Publishing LLC*. [http://dx.doi.org/10.1063/1.4818156]

I. INTRODUCTION

Branched conjugated oligomers and their derivatives represent a class of promising new photovoltaic materials with numerous applications due to their interesting electronic and photo-physical properties,[1–16] as well as the ability to modify the molecular geometrical structure in a variety of ways.[5,17,18] Molecular design of branched conjugated structures with desired optoelectronic properties requires theoretical interpretation and modeling of their electronic spectra. However, commonly used quantum chemical methodologies are not suitable for the direct implementation as an efficient spectroscopic tool due to the large molecular size and the complexity of the excited state electronic structures in conjugated systems,[19] the latter originating from the delocalized nature of the π-electron system, absence of symmetries, strong Coulomb correlations, and electron-phonon interactions, the latter two leading to particularly strong effects in low-dimensional geometries.[20] To address the above challenges, the exciton scattering (ES) approach has been recently developed that allows for efficient spectroscopic calculations in large branched conjugated molecules.[20–22]

Within the ES picture, a branched conjugated molecule/structure is viewed as a quasi-one-dimensional system, whose geometry is described by a graph with its edges and vertices representing the molecular linear segments and branching centers, respectively. In other words, the linear segments represent finite size pieces (oligomers) of a backbone polymer, while the branching centers stand for molecule termini, including chemical substitutions, and various kinds of joints, e.g., benzene rings that connect together two, three, or four linear segments. Electronic excitations in conjugated molecules are viewed as quantum quasiparticles (excitons) that move along the linear segments as free particles, being scattered at the vertices. As a result of exciton motion along the segments and its scattering at the vertices, a standing wave is formed that adequately represents an electronic excitation, provided scattering is short range, and the linear segment is long compared to the scattering length scale, the latter being of the order of the exciton size (i.e., a typical distance between an electron and a hole in the excitation). Stated equivalently, an electronic excitation is represented by a standing wave, represented by a pair of plane waves on each linear segment, whose amplitudes are established dynamically as a result of their propagation along the segments (graph edges) and scattering at the branching centers (graph vertices). Therefore, the molecular building blocks, i.e., the linear segments and branching centers can be characterized by the exciton dispersion $\omega(k)$ and exciton scattering matrices $\Gamma(\omega)$, respectively. The exciton dispersion describes the dependence of the exciton energy ω on its quasimomentum k in an infinitely long polymer that possesses discrete translational symmetry. The exciton dispersion describes the exciton motion on linear segments at distances from the branching centers that exceed the exciton size, where the deviation of the exciton center-of-mass wavefunction from a linear superposition of two plane waves is negligible. Therefore, $\omega(k)$ is property of the repeat unit of the backbone polymer. A branching center that connects n linear segments, and referred to as a vertex of degree n, is characterized by an $n \times n$ ($n = 1$ for the termini,

a)serg@lanl.gov
b)chernyak@chem.wayne.edu

 © 2013 AIP Publishing LLC

This article is copyrighted as indicated in the article. Reuse of AIP content is subject to the terms at: http://scitation.aip.org/termsconditions. Downloaded to IP: 192.12.184.6 On: Mon, 25 Aug 2014 22:50:00

$n = 2$ for double joints, $n = 3$ for triple joints, and so forth) frequency-dependent scattering matrix $\Gamma(\omega)$ that expresses the n amplitudes of the outgoing plane waves in terms of the incoming counterparts. Therefore, $\Gamma(\omega)$ is the property of a branching (scattering) center and the backbone polymer.

In the series of publications,[20–29] we have developed the ES theory as an efficient and accurate tool for computation of electronic excitations in branched conjugated molecules with perfect molecular geometries. The latter means that the existence of the scattering centers is the only source of violation of the translational symmetry in the linear polymers, which allows to use a plane wave approximation far away from the scattering centers. The exciton spectra and frequency-dependent scattering matrices, referred to as the energy parameters, totally characterize the molecular building blocks in terms of the excitation energies. Efficient computation of the oscillator strengths associated with optical transitions require some additional characterization in terms of so-called spectroscopic parameters, that characterize the contributions of the repeat units and scattering centers to the transition dipoles and transition charges, associated with electronic transitions. The energy parameters are retrieved from reference quantum chemical calculations in molecular fragments of relatively small size (linear segments, including the ones with donor/acceptor substitutions, and scattering centers with linear segments of moderate size attached). Once the above parameters are retrieved, the excited states can be found with minor numerical effort by solving a generalized "particle in a box" problem on the corresponding graph, with the scattering matrices playing the role of the actual, rather than phenomenological, boundary conditions. In the limit $l_e \ll L$ when the exciton size is short compared to the typical size L of a linear segment, the ES approach is asymptotically exact, however, as we have demonstrated,[20–29] it works with amazing accuracy in the case of relatively short linear branches, which just exceed the exciton size, the latter fortunately being restricted to 1–3 repeat units. In our previous work, we have characterized the exciton spectra for the phenylacetylene backbone and a variety of scattering centers, including neutral (hydrogen atom), as well as donor/acceptor substituted termini, and some symmetric double, triple, and quadruple joints, whose scattering matrices have been parameterized via the relevant scattering phases according to the geometrical symmetries.[28]

However, the ES method, being based on the plane wave picture of the excitations in regions not too close to the scattering centers, apparently fails, once the molecule geometry is distorted. On the other hand, understanding the electronic structure as a function of molecular geometry is crucial in describing the effects of static disorder and exciton-phonon coupling. In particular, this dependence actually describes the coupling between the electronic and vibrational motions and being characterized could lead to an efficient parameterization of an exciton-phonon Hamiltonian, similar to the ones used for Frenkel excitons. A natural way to accomplish this challenging task is to try to describe the excited state electronic structure, or in other words the exciton properties, in terms of a moderately small number of parameters, followed by identifying the dependence of these parameters on the molecular geometry, which should result in an exciton-phonon Hamiltonian, which would map the problem of incoherent energy transfer and relaxation in electronically excited states to its Frenkel exciton counterpart. The latter problem is still complex, however, it is substantially, if not infinitely, simpler than the problem of incoherent dynamics of a large conjugated structure with delocalized π-electron system and strong electron correlations.

The simplest and most intuitive way to parameterize the exciton properties would be introducing a tight-binding model that describes the exciton center-of-mass motion, assuming that the exciton center-of-mass can reside on a number of sites that represent the repeat units and scattering centers (with possibly more than one site per repeat unit or scattering center). Our previous results reveal that the exciton dispersions $\omega(k)$ retrieved from quantum-chemical computations can be well approximated by a small number of harmonics, which indicates potential application of lattice (tight-binding) models, mentioned above, with short-range hopping. The latter reflects strong electron correlations in organic conjugated systems that result in small exciton size up to a few repeat units, which suggests that the molecular vertices could also be described within an effective lattice model. Within such an approach the ES methodology is used in an indirect way, however, still playing a crucial role. The exciton spectra and frequency-dependent scattering matrices become a benchmark for building the tight-binding model. More specifically when representing the repeat units and scattering centers using certain numbers of sites, we will be identifying the values of the model parameters, such as on-site energies and hopping constants by requiring that the exciton spectra and scattering matrices obtained in a tight-binding models reproduce their counterparts, retrieved from quantum chemical computations. Stated differently, the ES approach serves as a necessary bridge between the quantum-chemical methods and the efficient tight-binding description of the electronic excitations. It helps in determining the morphology and parameters of the effective lattice for the optimized geometry, with a further goal of identifying the dependence of the tight-binding model parameters on the geometry distortions. In this manuscript, we focus on building adequate lattice models in the case of ideal molecular geometries, treating it as the first, still necessary step on the way of building Frenkel-type exciton-phonon Hamiltonians.

The task of building the tight-binding models becomes much easier, if one implements the study of analytical and topological properties of the scattering matrices, associated with the scattering centers. Our preliminary studies show that the above properties are most naturally formulated by replacing the frequency dependence of the scattering matrices with its quasimomentum dependence, which is naturally obtained using the exciton spectrum $\omega(k)$, which results in the scattering matrices $\Gamma(k)$.

The analytical and topological properties of the scattering matrices obtained from the ES approach can be imposed as an important criterion to select decent lattice models. Thus, the dependence of the scattering matrices can be attributed to a limited number of lattice model parameters. The analytical expressions of the scattering matrices derived from a lattice

This article is copyrighted as indicated in the article. Reuse of AIP content is subject to the terms at: http://scitation.aip.org/termsconditions. Downloaded to IP: 192.12.184.6 On: Mon, 25 Aug 2014 22:50:00

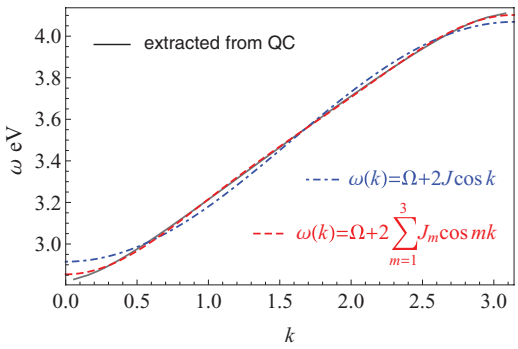

FIG. 1. The extracted exciton dispersion from time-dependent Hartree-Fock (CEO[31–34]) energies fitted with one and three cosines, where Ω and J represent the on-site energy and the hopping constant, respectively, in the infinite linear chain.

model allow us to do analytic continuation to predict the positions of bound states regarding to the scattering phases.

The manuscript is organized as follows: We first generalize the morphology of tight-binding models based on the exciton scattering analysis and formulate general tight-binding equations. In Sec. III, the simplest tight-binding model for linear molecules has been discussed by characterizing the exciton reflection. Finally, the representation of tight-binding models has been applied to excitons of particular type on molecular termini, double joints, symmetric triple and quadruple branching centers. The resonant states and bound states incorporated within the tight-binding models are discussed in Sec. IV.

II. EFFECTIVE TIGHT-BINDING REPRESENTATION OF EXCITON STATES

According to our previous studies of the exciton scattering in branched conjugated molecules, and as mention in Sec. I, we know that the size of light (i.e., the lowest energy band) excitons in phenylacetylene (PA) oligomers is about 1–3 repeat units due to the delocalized π-electrons subjected to strong electronic correlations.[22] This fact is also confirmed by the expansion of the exciton dispersion $\omega(k)$ [that satisfies the property $\omega(-k) = \omega(k)$ due to time-reversal symmetry], retrieved from quantum-chemical computations, and represented using Fourier series in terms of quasimomentum k (see Figure 1). The exciton dispersion can be adequately described by a limited number of cosine modes, which coincides with the one obtained in a tight-binding (lattice) models with nearby hopping. Stated equivalently, the excitons of a particular type (band), in terms of their motion along the linear segments, can be described using a tight-binding model with one site per repeat unit. Description of the scattering centers within the lattice model approach is more involved, since it is unknown in advance how many sites are needed to describe a particular center. Therefore, we set the stage with introducing a lattice model of a general type, and further describe how to determine its morphology and the parameters using the concept of the scattering matrices, and, in particular their topological and analytical properties, discussed in some detail in Refs. 22, 27, 28, and 30.

A tight-binding model that describes electronic excitations (excitons) in a branched PA molecule is defined on a graph (i.e., an irregular lattice) as shown in Figure 2. A repeat unit, centered at triple bond, is represented by a single site, whereas the molecular vertices (i.e., termini with and without substituent, meta joint, and symmetric quadruple joint) are generally represented by combinations (subgraphs) of linked sites, whose number has to be determined, as briefly discussed above. An excitation is described by its wave function φ, whose components φ_a reside at the sites a of the tight-binding graph, that is identified as an eigenstate $\hat{H}\varphi = \omega\varphi$ of the tight-binding Hamiltonian with the diagonal elements $H_{aa} = \Omega_a$ and off-diagonal elements $H_{ab} = J_{ab}$, referred to as the on-site energies and hopping constants, respectively.

The Hamiltonian of a lattice model can be conveniently recast in its second, quantized form,

$$H \equiv \sum_m \Omega_m B_m^\dagger B_m + \sum_{m,n}^{n\neq m} J_{mn} B_m^\dagger B_n, \qquad (1)$$

where $B_m^\dagger$ and B_m are creation and annihilation operators of an excitation on site m, respectively, which satisfy the canonical boson commutation relation. The Hamiltonian in Eq. (1) is reminiscent of the Frenkel-exciton Hamiltonian[35,36] that describes a collection of chromophores with no charge transfer between them, where with Ω_m and J_{mn} representing the chromophore transition energies and coherent hopping constants, respectively, the latter describing the Coulomb interactions between the transition charge distributions associated with the corresponding chromophores. At this point, we want to emphasize that although the tight-binding Hamiltonian [Eq. (1)] looks exactly like the Frenkel-exciton counterpart, the excitations under study are charge-transfer, rather than Frenkel excitons, and hopping processes, described by J_{mn} are dominated by exchange, rather than direct Coulomb interactions. Such strong exchange interactions appear due to strong electron-correlation effects characteristic for such low-dimensional

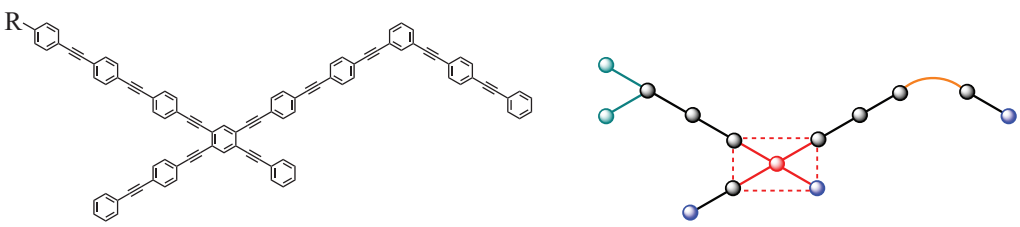

FIG. 2. A conjugated molecule and the corresponding graph of a possible tight-binding model. Different colors of sites and links represent different on-site energies and hopping constants.

This article is copyrighted as indicated in the article. Reuse of AIP content is subject to the terms at: http://scitation.aip.org/termsconditions. Downloaded to IP: 192.12.184.6 On: Mon, 25 Aug 2014 22:50:00

organic semiconductors with delocalized π-electronic states. Therefore, the hopping constants in our case are the sub-eV range, rather than several hundred wave numbers, as in the case of molecular aggregates. It should be also emphasized that at this juncture the ES approach is developed on the level of one-(quasi)particle states. This allows linear response, as well as energy transfer to be treated efficiently. In our future work we plan to extend the ES method to optical nonlinearities by studying the exciton-exciton scattering matrices. This will allow in particular to address the type of exciton statistics, which will show up in the commutations relations of the exciton creation and annihilation operators. On the other hand, a description of strongly correlated charge-transfer excitons in terms of Frenkel-exciton Hamiltonian reduces the problem to a much simpler one, as well as allows the methodology, developed over the decades in the context of Frenkel excitons, to be applied to our originally much more complex case. The latter is of special importance for describing incoherent processes due to energetic disorder and exciton-phonon coupling. However, as already briefly stated in Sec. I, building the exciton-phonon Hamiltonian goes beyond the scope of the present manuscript and will be addressed somewhere.

An eigenstate

$$|\Psi_j\rangle = \sum_n \Psi_j(n)|n\rangle, \tag{2}$$

of the tight-binding Hamiltonian in the case of an infinite linear chain with perfect geometry, or, stated equivalently, discrete translational symmetry, when the on-site energy $\Omega_m = \omega_0$ is a constant, whereas the hopping constants $J_{mn} = \bar{J}_{|m-n|}$ depend only on the distance between the corresponding sites, satisfies the Schrödinger equation of a form,

$$\sum_d J_d \left(\Psi(n-d) + \Psi(n+d)\right) = (\omega - \omega_0)\Psi(n), \tag{3}$$

where integer d and n denote the hopping distance and the lattice site label, respectively, and has a plane-wave solution,

$$\Psi_k(n) = Ae^{ikn}, \quad \omega(k) = \omega_0 + 2\sum_d \bar{J}_d \cos(dk), \tag{4}$$

with $\omega(k)$ being the exciton dispersion (spectrum), as the dependence of its energy ω on the quasimomentum k. Note that Eq. (4) describes the exciton dispersion in a form of a Fourier series, and expresses the exciton band width in terms of the hopping constants $\bar{J}_d$, and indicates the center of the exciton band and the bandwidth to be ω_0 and $4\bar{J} = 4\bar{J}_1$ in case of nearest neighbor hopping. Obviously the number of significant cosine harmonics in the Fourier expansion specifies the allowed hopping distance d.

Summarizing, the tight-binding representation of an infinite polymer can be obtained in a relatively easy and natural way by introducing a lattice site per repeat unit, followed by identifying the "central" frequency ω_0 and the hopping constants $\bar{J}_d$ using the Fourier series expansion of the spectrum $\omega(k)$, retrieved from quantum chemistry calculations, the latter described in detail in our previous work on the ES approach.

Finding the tight binding representation of the molecular scattering centers is conceptually straightforward, once the ES approach is developed: one needs to find such a representation that the scattering matrix $\Gamma(\omega)$ in the lattice model adequately reproduces the one retrieved from quantum chemistry computations. Within a lattice model, $\Gamma(\omega)$ can be computed analytically by finding the solution of the Schrödinger equation at energy ω with a single incoming wave at large enough distance from the scattering center, where the wavefunction is represented by a superposition of generally two plane waves (moving in opposite directions). The result of the above computation is explicit in terms of products and inverses of certain $n \times n$ matrices, where n is the number of lattice sites that represent the scattering center. However, such fitting is not an easy task for practical implementations, especially when a relatively large number of sites are required to represent a scattering center, and it is desirable to develop certain principles that would allow to narrow our search for the tight-binding representations.

The above principles are based on the topological and analytical properties of the scattering matrices, observed and discussed in some detail in our previous work.[22,27,28,30] The topological analysis of a scattering matrix $\Gamma(\omega)$, retrieved from quantum chemistry computations, allows to identify the number of lattice sites that represent the corresponding scattering center, which provide a huge simplification. Studying the analytical properties provides with an extremely helpful insight on the structure of the tight-binding model parameters, i.e., on-site energies and hopping constants, associated with the sites, representing the scattering center.

The topological analysis is based on counting the number of excited states in a finite branched molecule. In a real molecule of finite size, molecular vertices violate the discrete translational symmetry of the polymer chain, causing exciton scattering and consequently standing wave formation, which makes the quasimomentum k quantize, i.e., attain a discrete, and in our case finite, set of values. The number of states in a lattice model is obviously given by the total number of lattice sites. It is also intuitive that a lattice site representing a repeat unit of the backbone polymer provides a state in a lattice model, and a quantum chemistry calculation, respectively. Therefore, the number of the lattice sites that represent a scattering center should be given by the number of additional states the above scattering center "brings to the table," provided the latter concept can be formalized in some way.

The aforementioned formalization was initially obtained for scattering centers of degree 1, i.e., molecular termini, including donor-acceptor substituted, by counting the number of exciton states in linear oligomers.[28] The topological analysis was based on considering the scattering matrix as the function of quasimomentum k, by making use of the exciton dispersion law, i.e., setting $\Gamma(k) = \Gamma(\omega(k))$, and making use of an obvious fact that the scattering matrix of a terminal is a 1×1 unitary matrix, i.e., a unimodular complex number $\Gamma(k)$ that naturally resides on a unit circle in complex plane and depends on quasimomentum k that resides in the 1D Brillouin zone, and, therefore, also resides on a unit circle. Therefore, the scattering matrix $\Gamma^{(A)}(k) = e^{i\phi(k)}$, associated with the terminal A, is given by a map from a unit circle to a unit circle, and possesses an integer-valued topological invariant m_A, referred to as the winding number (or more precisely the degree

This article is copyrighted as indicated in the article. Reuse of AIP content is subject to the terms at: http://scitation.aip.org/termsconditions. Downloaded to IP: 192.12.184.6 On: Mon, 25 Aug 2014 22:50:00

of the map) that provides the number of times $\Gamma(k)$ winds over its unit circle of residence, while the quasimomentum goes once over the Brillouin zone.

The number of solutions of the ES equations was further identified with a number of intersections of two curves on a 2D torus (which is natural, since in a way the solutions (with real values of k) of systems of equations can be also interpreted as intersections of certain graphs of functions), with the latter being estimated using topological intersection theory as

$$N \geq L + Q_A + Q_B, \tag{5}$$

where L is the segment length (strictly speaking the number of repeat units), Q_A and Q_B are the topological charges of the two termini, related to the corresponding winding numbers by

$$Q = (m-1)/2, \tag{6}$$

with the bound in Eq. (5) becoming tight for long enough segments. The factor 1/2 in Eq. (6) reflects the fact that one excited state is represented by two values $\pm k$ of quasimomentum, whereas $(m-1)$ reflects the fact that $k = 0, \pi$ corresponds to non-physical (i.e., completely zero) solutions of the ES equations. Note that, as noted above, Eq. (5) counts the number of solutions of the ES equations with real values of k, i.e., with the energies located inside the exciton band, whereas the bound states, localized in some region around the scattering center, have energies outside the exciton band. Therefore, the number of lattice sites that represent a scattering center A is equal to $Q_A + \bar{Q}_A$, where $\bar{Q}_A$ represents the number of bound states in a molecule that contains a scattering center A with a long enough linear segments attached to it. In Ref. 28, we have also made use of spatial symmetry to extend Eq. (5) to the case of molecules that consist of a symmetric joint with the linear segment of identical size, completed by identical termini (with the latter two conditions necessary for the molecule to maintain the symmetry of the joint).

The topological counting formula that extends Eq. (5) to the case of arbitrary branched molecules with arbitrary, not necessarily symmetric joints, has been derived in Ref. 30 by formulating the ES equations on an arbitrary graph as an intersection problem, followed by applying the topological intersection theory in a much more non-trivial setting. Therefore, we are not describing any details here, directing the reader, interested in those details, to Ref. 30, restricting ourselves to the statement that the index theorem presented in Ref. 30 supports the concept of the states, "brought up to the table" by a scattering center in the case of a branched molecule of arbitrary morphology, as well as describes the winding number and topological charge of an arbitrary joint, reproducing in particular cases of molecular termini and symmetric joints the simple expressions, obtained in Ref. 28. Therefore, in this manuscript that involves symmetric joints only, we will refer to the simple expressions for topological charges, obtained in Ref. 28. We will just mention for the sake of completeness that the winding number m_A of an arbitrary joint is given by the winding number of the map $\det \Gamma(k)$ of the Brillouin zone to a unit circle, since the determinant of a unitary matrix is given by a unimodular number.

While studying the topological properties of the scattering centers, namely, the topological charges, solves an important problem of identification of the number of sites in the corresponding tight-binding model that represent the center, knowing the analytical properties of the scattering matrix provides with detailed insight in terms of the lattice model parameters that should be used to represent the corresponding joint. As noticed in our previous work,[22,27,28] an electronic state of a joint alone, whose energy lies inside the exciton band, being weakly coupled to the excitons that reside on any attached infinitely long linear segment, results in a sharp dependence of the scattering matrix on frequency in the region centered at the joint's state energy with the energy width characterized by the coupling strength, so that $\det \Gamma(\omega)$ acquires the phase of 2π. The latter naturally changes the scattering center topological charge by 1, which is consistent with the topological analysis. Weak coupling to excitons of a joint's state with the energy outside the exciton band results in a bound state, which corresponds to a zero/pole in the analytical continuation of $\det \Gamma(k)$ to complex values of k. If the bound state energy is close to the band edge, this will result in the sharp dependence on k of the scattering phases in the vicinity of the band edge. We will see examples of such behavior in Secs. III and IV.

III. SIMPLE TIGHT-BINDING MODEL

In this section, we introduce and study the simplest tight-binding model that describes electronic excitations (excitons) in linear PA molecules. The considered tight-binding model represents a molecular terminus, and nearby repeat units are shown in Figure 3. Only nearest-neighbor hopping J_1 is considered for the sake of simplicity. The molecular terminus is described by modification of its on-site energy (ω_1, instead of ω_0 for the repeat units). Generally speaking one can consider a more general lattice model by also modifying the hopping constant between the lattice sites that represent the terminus and the first repeat unit; this will be discussed later in this section after obtaining the simplest possible analytical expression. The exciton dispersion relation adopts a form $\omega(k) = \omega_0 + 2J_1 \cos k$, so that the exciton energies are in the range $\omega_0 \pm 2J_1$. The exciton wave function is given by a superposition of two plane waves propagating in opposite directions

$$\Psi(n) = r_0(k)e^{ikn} + e^{-ikn}, \tag{7}$$

where $r_0(k)$ is the reflection amplitude with respect to the reference point $n = 0$. Note that the reflection coefficient is sensitive to the reference point choice: it acquires the phase shift of $2\,mk$ when the reference point of the reflection is shifted by m.

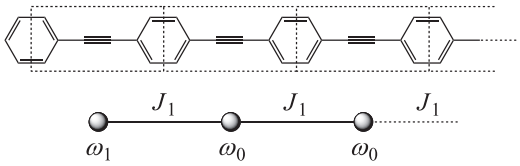

FIG. 3. The simplest tight-binding model for excitations near molecular termini of PA oligomers.

This article is copyrighted as indicated in the article. Reuse of AIP content is subject to the terms at: http://scitation.aip.org/termsconditions. Downloaded to IP: 192.12.184.6 On: Mon, 25 Aug 2014 22:50:00

Therefore, the reflection amplitude $r(k)$ defined with respect to the reference point $n = 1/2$ in the previous ES publications is found to be $r(k) = r_0(k)e^{ik}$.[28]

For our simplest lattice model, in which only the on-site energy of the site that represents the terminus is modified, applying the lattice equation [Eq. (3)] to the modified site $n = 1$, results in the following explicit expression for the reflection amplitude:

$$r(k) = -e^{ik}\frac{ge^{-ik} + 1}{ge^{ik} + 1}, \tag{8}$$

with $g = -(\omega_1 - \omega_0)/J_1$.

A bound state localized in the vicinity of the terminus corresponds to a complex value of the quasimomentum, so that $|e^{-ik}| < 1$, and the wavefunction associated with the bound state decays exponentially in the linear segment, provided the reflection coefficient $r(k) = 0$. Note that this is a particular case of general quantum scattering theory that identifies the bound state as the zeros of the scattering matrix analytically continued to the complex values of the momentum/energy. The condition $r(k) = 0$ results in

$$\omega_{b.s.} = \omega_0 - J_1(g + g^{-1}). \tag{9}$$

Therefore, the bound state exists when $|g| > 1$, i.e., the modification of the on-site energy on the site that represents the terminus $|\omega_1 - \omega_0|$ exceeds the coupling strength, which is a quarter of the exciton band width. For negative and positive g, considering J_1 being negative, the bound state can be either below or above the exciton band, respectively. In other words, the tight-binding representation of the reflection amplitude allows for analytic continuation of $r(k)$ to complex value of k, which allows the bound exciton state to be identified whose energy is outside the exciton band. Figure 4 shows possible shapes of the reflection phase when the terminus is characterized by just modification of the on-site energy. The relation between the topological charge Q of the phase and the parameter g has been clearly described in the figure caption.

The change of the value of the terminus topological charge by 1 when g goes through the value $|g| = 1$ is obvious, still worth commenting on. The change of g does not change the fact that the terminal provides an additional excited state. It shows as a bound state in the case $|g| > 1$, or as an additional state inside the exciton band for $|g| < 1$, when the bound state does not exist, which results in an increase of Q by one, in the full agreement with the topological counting formula.

The example, considered in this section, demonstrates that even the simplest tight-binding model is capable of qualitative description of the exciton scattering at molecular vertices. The exciton dispersion $\omega(k)$, which characterizes infinite linear segments, is parameterized by two constants, the on-site energy ω_0 and the nearest neighbor hopping constant J_1. The energy-dependent reflection phase ϕ_T, that describes molecular termini in the ES approach, is replaced by the geometry-related lattice constant ω_1, so that the description of the electronic excitations in conjugated molecules is even more simplified. The investigation on geometry-dependent electronic excitations becomes practicable using tight-binding models.

In the remainder of this section, we extend the lattice model, studied earlier, by allowing also the hopping constant between the first and second sites, denoted J_0 to be modified in order to better describe the terminus effect, e.g., resonant states introduced by chemical substitution. By imposing the lattice equation [Eq. (3)] to sites $n = 1$ and $n = 2$, which are connected via J_0, the reflection amplitude is found to be

$$r(k) = -e^{ik}\frac{(ge^{-ik} + 1) + e^{-2ik}(1 - q^2)}{(ge^{ik} + 1) + e^{2ik}(1 - q^2)}, \tag{10}$$

with $q = J_0/J_1$.

Modification of the hopping constant in addition to the on-site energy allows for more flexible simulation of the reflection phase, as well as illustrating additional qualitative features, such as weak coupling of a state, localized on the terminus to the exciton band. For given value of g that describes the energy position of the state localized at site $n = 1$ with respect to the exciton band, the hopping constant J_0 controls the coupling strength between the two, and, therefore, dramatically affects the shape of the scattering phase.

In Figure 5, we present the reflection phase as a function of quasimomentum for four sets of parameters (g, q); in all cases there is no bound state. Therefore, in all cases the topological charge $Q = 0$, which reflects the fact that for long enough linear segments, all exciton energies are inside the band, supporting the no-bound-state scenario. However, the shapes, including the ways how the topological charge is accumulated over the Brillouin zone, are very different, depending on whether the coupling J_0 is small or not, which

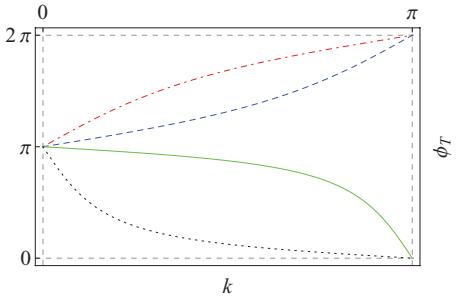

FIG. 4. Possible shapes of the reflection phase at the terminus characterized by modification of just the on-site energy with the nearest neighbor hopping in the chain, for four values of g: −0.3 (red dotted-dashed), 0.3 (blue dashed), 1.5 (green solid), and −1.5 (black dotted). The topological charge $Q = 0$ if $|g| < 1$, $Q = -1$ if $|g| > 1$.

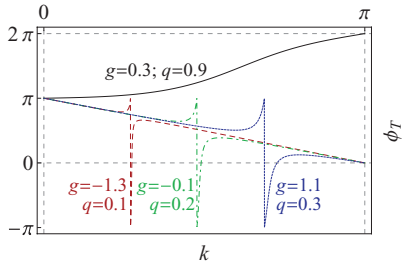

FIG. 5. Possible shapes of the reflection phase at the terminus characterized by modification of one on-site energy and one hopping constant with the nearest neighbor hopping in the chain, correspond to different values of g and q.

This article is copyrighted as indicated in the article. Reuse of AIP content is subject to the terms at: http://scitation.aip.org/termsconditions. Downloaded to IP: 192.12.184.6 On: Mon, 25 Aug 2014 22:50:00

corresponds to $q \ll 1$, and $q \sim 1$, respectively. In the case $q = 0.9$ and $g = 0.3$, which is close to $q = 1$ that corresponds to the simplest model, the phase shows similar behavior (compare with the case g = 0.3 shown in Figure 4) of going monotonically from 0 to π over half of the Brillouin zone. In the three other cases that correspond to the weak coupling limit, the behavior is quite different. For most values of k, the phase shows monotonic and actually linear decreasing behavior (that corresponds to no coupling limit) with sharp features, referred to as phase kinks or resonances, where the phase changes by 2π over a narrow region of quasimomenta, which results in the same $Q = 0$ value of the topological charge, accumulated, however, in a very different way. For weak coupling, the resonant feature occurs when ω_1 is located inside the exciton band ($|g| < 2$), and its position in the quasimomentum space is naturally determined by the condition $\omega(k) = \omega_1$. The resonance width is determined by q, so that the resonances are becoming sharper with the coupling constant J_0 tending to zero.

To analyze the kink shape in the weak coupling $q \to 0$ limit, we introduce a variable $z = e^{ik}$, so that for real values of k we have $|z| = 1$ and recast the expression for the reflection amplitude [Eq. (10)] in a form

$$r(z) = -\frac{1}{z}\frac{(z^2 + gz + 1) - q^2}{(z^2 + gz + 1) - q^2 z^2}, \tag{11}$$

with the term in the parenthesis turning to zero for $z = z_0$ with

$$z_0 = -\frac{g}{2} \pm i\frac{\sqrt{4 - g^2}}{2}. \tag{12}$$

For small values of q, we can neglect the $\sim q^2$ terms in the numerator and denominator in the rhs of Eq. (11), as long as z is not close to z_0, which results in $r(z) \approx -(1/z)$ that corresponds to the decoupled case and represented by the monotonic linear decrease of the scattering phase from π to 0, apart from the resonant features, as clearly shown in Figure 5. To analyze the phase kinks (resonances), we represent $z = z_0 + \xi$, and expanding the numerator and denominator in Eq. (11) up to linear terms in ξ, we obtain

$$r(\xi) = -\frac{1}{z_0}\frac{\xi - i\gamma}{\xi - z_0^2 i\gamma}, \quad \gamma = \frac{2q^2}{\sqrt{4 - g^2}}. \tag{13}$$

It follows from Eq. (13) that $r(z)$ has a zero and a pole, located close to z_0, inside and outside of the circle $|z| = 1$, symmetrically with respect to the aforementioned circle with the distance between the zero and the pole $|\Delta z| \approx q^2$, which implies the resonance width to be $\Delta k \sim q^2$. Note that the resonance width depends on the ratio q of the couplings only, being independent of the resonance position.

Summarizing, a simple tight-binding model with only two parameters ω_1 and J_0 describing the corresponding terminus, is capable of representing various physical phenomena, including formation of bound and resonant states, having control of their positions and phase kink sizes, associated with the phase kinks.

IV. TIGHT-BINDING MODELS FOR EXCITONS IN PA-BASED BRANCHED STRUCTURES

Based on the ES method, the tight-binding model approach is expected to be accurate and efficient, being applied to any exciton band that describes excitons of relatively small size. By inspecting the transition density matrices obtained from quantum-chemical computations, using the collective electronic oscillator (CEO) method,[31–34] we can single out the lowest-energy exciton band, whose band width is around 1 eV, referred to as delocalized or light exciton band.[24] In this section, we develop the tight-binding model that describes propagation and scattering of excitons that belong to the light exciton band in PA-based molecules.

Although the dispersion curve for light excitons can be qualitatively described by the nearest-neighbor hopping, to achieve high accuracy one would need overall three cosine Fourier modes, which restricts the hopping distance to three repeat units (up to third neighbor hopping). Using the notation introduced in Eq. (4), the exciton dispersion is described by

$$\omega(k) = \omega_0 + 2\bar{J}_1 \cos k + 2\bar{J}_2 \cos 2k + 2\bar{J}_3 \cos 3k, \tag{14}$$

with $\omega_0 = 3.49052$ eV, $J_1 = -0.29303$ eV, $J_2 = -0.00618$ eV, and $J_3 = -0.01847$ eV. The above values of the hopping parameters are obtained from the best fit of the dispersion relation extracted from quantum-chemical results, as shown in Figure 1. Formally for a given energy ω Eq. (14) has three pairs $\pm k$ of solutions for the quasimomentum. However, in the energy range of interest, i.e., inside and around the light exciton band, due to $|J_2|, |J_3| \ll |J_1|$, only one pair is relevant, namely, the one that represents a weak correction, induced by J_2 and J_3 to the nearest-neighbor solution. Therefore, the excitation of given energy in the range of interest is still represented by standing waves with two plane waves with the quasimomenta $\pm k$ per linear segment.[38]

Tight-binding models with up to the third neighbor hopping provide higher accuracy in terms of the exciton dispersion relation, as well as allow for more versatile choice to characterize molecular vertices, compared to those with the nearest neighbor hopping, since there are more lattice parameters around the joint that can be varied. However, longer hopping distance makes the tight-binding models more difficult to be processed analytically, whereas the benefits of the increasing accuracy are not that pronounced, considering that the nearest neighbor hopping constant is still much larger than the other two. Therefore, a nearest-neighbor tight-binding model ($J_1 = -0.28783$ eV and $\omega_0 = 3.49207$ eV) has been applied to describe the light exciton band as well. By comparing the two tight-binding models, we observed that long range hopping does not remarkably affect the exciton scattering properties, the latter being adequately described by introducing more tight-binding parameters within a vertex, especially for those who show of complex features in the scattering matrices. Therefore, in what follows we present the results based on the nearest neighbor hopping tight-binding models.

This article is copyrighted as indicated in the article. Reuse of AIP content is subject to the terms at: http://scitation.aip.org/termsconditions. Downloaded to IP: 192.12.184.6 On: Mon, 25 Aug 2014 22:50:00

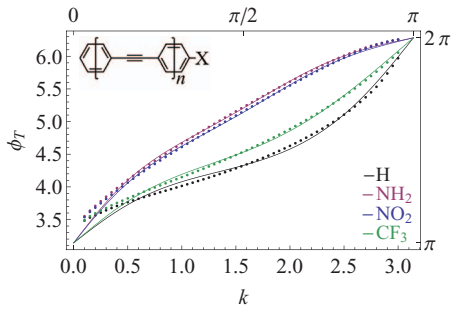

FIG. 6. Reflection phases of the four termini: (from bottom to top) unmodified phenyl ring, $-CF_3$, $-NO_2$, and $-NH_2$ substituted termini. The results of exciton scattering analysis on quantum-chemical computation are shown as dots, whereas the curves are the best fits using the nearest-neighbor-hopping tight-binding model. Inset: Linear PA oligomers with a substituent X (X = $-CF_3$, $-NO_2$, and $-NH_2$) on one end, which are used to extract the modified reflection phases.

A. Tight-binding models for molecular termini

In this section, we develop the tight-binding representation for the molecular termini, including substituents, represented by $–NH_2$, $–CF_3$, or $–NO_2$, connected to a phenylacetylene oligomer via in the para-position of the phenyl ring (see inset of Fig. 6). The dispersion relation $\omega(k)$ and the reflection phase $\phi_T(k)$ of the standard (neutral) termini have been extracted from quantum-chemical computations in linear molecules of different length, without substituents, using the relation $kL + \phi_T = \pi n$, where the integer n labels the excited states, with L being the molecule length.[24] The scattering phases $\phi_{D/A}$ of the modified termini can be then readily retrieved from quantum-chemical computations in linear molecules with one end being substituted, using the relations $2kL + \phi_T + \phi_{D/A} = 2\pi n$.[27] The reflection phases for all four termini under study are shown in Figure 6.

The morphology of a tight-binding model can be determined by inspecting the exciton scattering properties. In particular, the number of lattice needed to represent a vertex is directly related to its topological and analytical properties, as described in some detail in Sec. II. The zero values $Q = 0$ of the topological charges in all four cases (as clearly seen from Fig. 6) indicate that the considered molecular termini do not contribute to the number of excitations in the exciton band. Therefore, the number of sites in the tight-binding model is identical to the number of repeat units in a linear molecule, i.e., no additional sites should be used to represent the terminal, the latter being characterized by just modification of three parameters: the on-site energies of the two adjacent sites, as well as the hopping constant between the two. The ES properties are reproduced with high accuracy using the tight-binding model introduced above, as clearly seen from Figure 6 that shows a comparison between the scattering phases obtained from quantum chemistry computations and their tight-binding model counterparts.

Summarizing, in the tight-binding representation for the considered donors/acceptors, the effect of chemical substitution on electronic excitations is characterized by the variation of the tight-binding parameters near the substituent, using the exciton scattering phase as a benchmark. In particular, smaller on-site energy and weaker coupling near the terminus result in the increase of the reflection phase, the latter being attributed to the extended conjugation, which results in the red shift of the optical absorption spectrum.[27] The tight-binding parameters that characterize molecular substituents can be tabulated and provide intuitive guidance for chemical modification of electronic conjugation in branched conjugated molecules.

B. Tight-binding models for symmetric branching centers

As described in some detail in Ref. 28, exciton scattering at the so-called symmetric branching centers, i.e., molecular vertices that possess high enough spatial symmetry, can be analyzed in terms of the corresponding scattering phases. A mathematical reason that stands behind that is that the scattering matrix $\Gamma(k)$ of such a center can be diagonalized in a quasimomentum independent basis set that corresponds to decomposing the vector space of incoming/outgoing waves in irreducible representations of the finite (point) group that describes spatial symmetry of the joint under consideration. In such a picture, the corresponding quasimomentum dependent scattering phases $\phi(k)$ can be viewed as that $e^{i\phi(k)}$ represents the k-dependent eigenvalues of $\Gamma(k)$. Therefore, $\det\Gamma(k) = \prod_j e^{i\phi_j}(k) = \exp(i\sum_j \phi_j(k))$, where $\phi_j(k)$ with $j = 1, \ldots, \deg\Gamma$ are the phases that fully describe the scattering matrix of a symmetric joint (note that some of the phases can coincide as functions of quasimomentum, due to symmetry, e.g., in the case of a symmetric Y-joint). This implies that the winding number and the topological charge of a vertex are given by the sum of the winding numbers and topological charges, respectively, associated with the phases. Therefore, first, the topological charges, associated with the separate phases $\phi_j(k)$, characterize the number of additional states of given symmetry provided by a symmetric molecular vertex, and, second, the topological/analytical properties of the scattering matrices $\Gamma(k)$ can be performed for separate phases separately by attaching to the vertex the linear segments of identical length, so that the obtained molecular fragment maintains the spatial symmetry of the joint, which maps the scattering problem to an effective problem of reflection from a molecular terminal. The latter circumstance not only simplifies the analysis, but also allows classification of the additional states provided by a symmetric center, according to their symmetry. Naturally, the tight-binding parameters that characterize a symmetric joint should maintain its symmetry and the corresponding lattice model should describe all scattering phases of the given joint simultaneously. In what follows, we will consider the double (V), triple (Y), and quadruple (X) joints, based on a benzene ring.

The scattering phases of a double meta (M) joint extracted from quantum-chemical results are shown in Figure 7. The topological charges Q_0^M and Q_1^M (the subscript denotes the symmetries that correspond to even and odd parities) of both phases are zero, which indicates that the number of the excitations within the exciton band is $L + 2Q_T + Q_0^M + Q_1^M = L$, where $Q_T = 0$ is the topological charge of the unmodified terminus and L is the molecular

This article is copyrighted as indicated in the article. Reuse of AIP content is subject to the terms at: http://scitation.aip.org/termsconditions. Downloaded to IP: 192.12.184.6 On: Mon, 25 Aug 2014 22:50:00

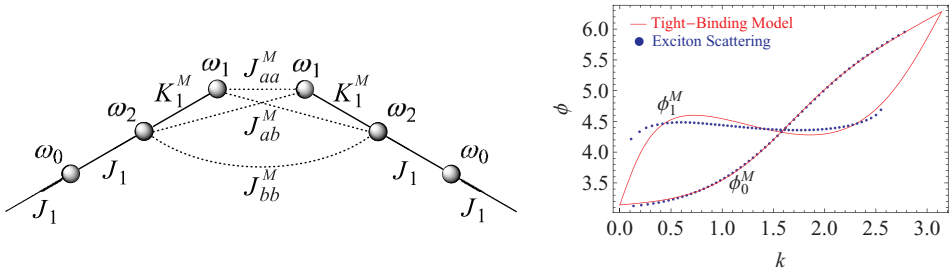

FIG. 7. (Upper) The tight-binding model has been used to describe the meta (M) joint. Dashed lines represent weak couplings. (Lower) The scattering phases of the meta (M) joint retrieved from the ES approach, which are approximated by the tight-binding model. Subscript 0/1 denotes scattering symmetries with respect to even and odd parities, respectively.

length. Since there is no excitations outside of the exciton band, the number of the sites N in the corresponding tight-binding model is equal to L. Therefore, each site in the model for a meta-conjugated molecule represents a repeat unit and no sites should be added for the joint. The meta-conjugation is described by modification of the on-site energies ω_1 and ω_2, the nearest neighbor hopping K_1^M, as well as adding three coupling constants J_{aa}^M, J_{ab}^M, and J_{bb}^M around the joint (see Fig. 7).

The coupling between the two repeat units connected via a meta joint is described by $J_{aa}^M = -0.01594$ eV, found from the best fits of the ES phases. The obtained value of the coupling J_{aa}^M is small, compared to the value $J_1 = -0.28783$ eV of the hopping constant in the chain, allows the weak coupling to be attributed to direct Coulomb interaction between the two linear segments, connected via a meta-joint, which agrees with the well-known inorganic chemistry impenetrable property of the meta-conjugated phenyl ring to block charge transfer. The other two hopping constants J_{ab}^M and J_{bb}^M allow the scattering phases to be reproduced with higher accuracy. Both are found to be weak, still comparable to J_{aa}^M. The latter circumstance supports the interpretation of the coupling in terms of direct Coulomb interaction that has long-range nature.

Exciton scattering at an ortho (O) joint has a resonant feature, seen in the symmetric (even parity) scattering phase ϕ_0^O (see Fig. 8), which has been missed in our analysis, presented in Ref. 28. Due to the values $Q_0^O = 1$ and $Q_1^O = 0$ of the topological charges, we conclude that the number of the exciton states in an ortho-conjugated molecule is $L + 1$,

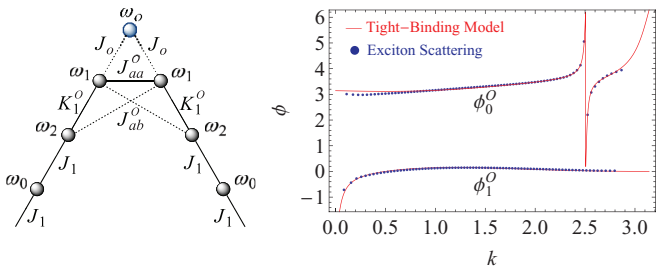

FIG. 8. (Upper) The tight-binding model that describes the ortho (O) joint. The joint is represented by an additional site with on-site energy ω_o. Dashed lines represent weak couplings. (Lower) The scattering phases of the ortho (O) joint retrieved from the ES approach, approximated by the tight-binding model. Subscript 0/1 denotes symmetric/antisymmetric (even/odd parity) phases that represent the scattering matrix.

L being the molecule length. Therefore, an additional lattice site should be introduced for a proper tight-binding characterization of the ortho joint. Being more specific, the effect of ortho-conjugation is described by an extra site with on-site energy ω_o, coupled to the two adjacent sites of the molecule with the hopping constant J_o, modification of the on-site energies of the aforementioned adjacent sites, and their nearest neighbors with ω_1 and ω_2, respectively, as well as modification and introduction of several hopping constants around the joint, as shown in Fig. 8.

Unlike the meta molecules, the coupling across the ortho joint between the two linked repeat units $J_{aa}^O = -0.27356$ eV is as strong as the coupling in linear chains $J_1 = -0.28783$ eV. This result indicates that ortho-conjugation is almost as transparent as para-conjugation. The sharp resonant feature, where the phase ϕ_0^O acquires an additional value of 2π over a narrow region of quasimomentum/energy, corresponds to an extra resonant state, whose energy has very weak dependence on the molecule length.[28] The above resonance can be interpreted as resulting from weak coupling of a state, localized at the joint to the exciton band. The position and the width of the resonance are determined by the on-site energy $\omega_o = 3.95661$ eV and hopping (coupling) constant $J_o = -0.02132$ eV, respectively. Both scattering phases that correspond to even and odd parities have been accurately described using the tight-binding model representation.

Following the same methodology, symmetric triple (Y) and quadruple (X) joints have been studied in terms of tight-binding models. No additional site has been used for the Y-joint since all its relevant topological charges are zero. Naturally, all parameters of tight-binding model are introduced or modified maintaining the joint symmetry. In each branch, the on-site energies of the two sites adjacent to the joint and the coupling strength between them are subject to modification. Intuitively, the inter-branch coupling in Y molecules can be introduced in the same way as for meta molecules. Hopping over distances less than two repeat units is also allowed between any two different branches. The hopping constants are referred to as J_{aa}^Y, J_{ab}^Y, and J_{bb}^Y, ordered by the relevant hopping distance (see Fig. 9).

Couplings between different branches are attributed to weak Coulomb interactions. Since interactions between sites linked by the Y-joint actually characterize meta-conjugation of a phenyl ring, the coupling strengths around Y-joint, as well as the modified on-site energies are similar to those that describe the double meta-joint, which agrees with the similarity

This article is copyrighted as indicated in the article. Reuse of AIP content is subject to the terms at: http://scitation.aip.org/termsconditions. Downloaded to IP: 192.12.184.6 On: Mon, 25 Aug 2014 22:50:00

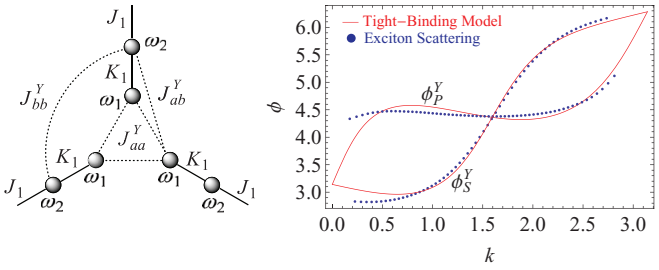

FIG. 9. (Upper) The tight-binding model for symmetric triple (Y) joint. Inter-branch hopping should be considered for any of two sites shown in the model. (Lower) The scattering phases of the Y-joint retrieved from the ES approach and approximated by the tight-binding model. Subscript S denotes the states where the angular momentum $m = 0$, whereas P denotes the double degeneracy of the $m = \pm 1$ modes.[28]

of the scattering phases, associated with the two (meta and triple) joints.[28]

The exciton behavior at the X-joint is more complicated because of the four distinct characteristic scattering phases with different topological charges (see Fig. 10): $Q = 0$ for ϕ_{11}, $Q = -1$ for ϕ_{01} and ϕ_{00}, $Q = 1$ for ϕ_{10}. A notation for the symmetry, as well as the analytical and topological analyses are specified in Ref. 28. The scattering with the A^1B^0 symmetry results in one additional resonant state in the exciton band, whereas the phases with symmetries A^0B^1 and A^0B^0 are responsible for the two bound states outside the band. Therefore, within a tight-binding model, the X-joint is represented by an additional site, with the on-site energy ω_x and the coupling strength J_x to the linked sites. In order to describe all four phases simultaneously, inter-branch coupling across the X-joint is allowed with the coupling distance along the molecule up to two repeat units. Two on-site energies and one hopping constant in the molecular branch in the vicinity of the joint are subject to modification, as shown in Figure 10.

The relevant lattice constants for the X-joint are obtained by fitting the exciton scattering phases retrieved from quantum chemistry using analytical expressions, provided by the lattice model. The sharp resonance feature of ϕ_{10} is attributed to the weak coupling $J_x = -0.02955$ eV between the additional site that represents the X-joint and the adjacent ones that represent the repeat units. The on-site energy $\omega_x = 3.46894$ eV matches the energy position of the resonant state. The coupling strengths across the X-joint also agree with the results obtained for just meta, ortho, and para conjugations. Specifically, weak couplings between the two branches linked via the meta-positions of X-joint have been obtained, in the full analogy with the case of a meta-joint, whereas the hopping constants $J_{aa}^{XP} = -0.27915$ eV and $J_{aa}^{XO} = -0.25711$ eV via the para and ortho positions, respectively, are similar to the nearest neighbor $J_1 = -0.28783$ eV and the ortho-conjugation $J_{aa}^{O} = -0.27356$ eV hopping constants, respectively.

Application of the tight-binding description for X-joint allows the bound exciton states, associated with the A^0B^1 and A^0B^0 symmetries to be predicted. Since the nearest neighbor hopping cannot accurately describe the exciton dispersion at the band edges, it appears reasonable to make a comparison with the quantum-chemical results using the bound state energy position relative to the exciton band, as opposed to comparing the absolute position of the bound state. The bound state with symmetry A^0B^1 predicted by the aforementioned lattice model is 151 meV below the lower band edge, compared to the CEO result of 78 meV. The bound state with symmetry A^0B^0 is predicted 5 meV above the exciton band with its CEO counterpart being missing due to the computational limitation. According to the analytical and topological analyses of the scattering phase and the trend for the highest excitation inside the band to be approaching the upper band edge with increasing the arm length, it is natural to expect that a bound state above the exciton band in the X molecules can be observed in the case of sufficiently long branches only.[28] This demonstrates capability of simple tight-binding representations to predict bound states in the close proximity of the band edges, via analytical continuations of the scattering matrix to complex values of k, when obtaining the aforementioned states through direct quantum chemistry becomes not feasible due to computational limitations.

V. CONCLUSIONS

In this paper, we introduced tight-binding (lattice) models to describe electronic excitations in conjugated molecules and structures. The lattice morphology and the model parameters (on-site energies and hopping constants) of the effective tight-binding models are identified by comparing the exciton dispersion and exciton scattering matrices at molecular termini, double joints, and branching centers, obtained within the lattice models with their counterparts, extracted from quantum-chemical computations. In particular,

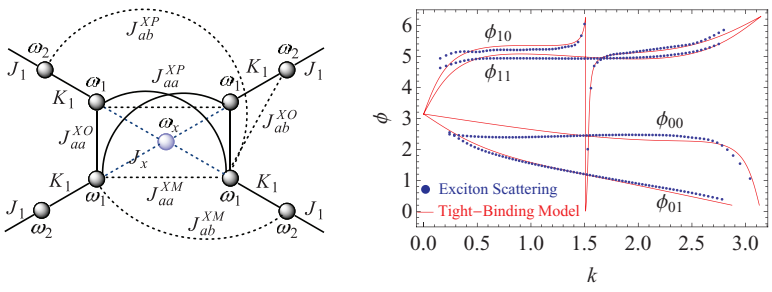

FIG. 10. (Upper) The tight-binding model for a symmetric quadruple (X) joint. (Lower) The scattering phases of the X-joint retrieved from the ES approach and fitted using the tight-binding model. Subscripts of the phases denote the symmetries of the exciton scattering processes.[28]

This article is copyrighted as indicated in the article. Reuse of AIP content is subject to the terms at: http://scitation.aip.org/termsconditions. Downloaded to IP: 192.12.184.6 On: Mon, 25 Aug 2014 22:50:00

the number of additional sites needed to represent a scattering center and connection of lattice sites (tight-binding model morphology) are determined by inspecting the topological and analytical properties of the scattering matrices, whereas the model parameters are obtained from the best fits of the scattering phases. The presented approach rests on making use of detailed quantum-chemical data, further processed using the exciton scattering method as an intermediate step, which distinguishes this work from numerous previous attempts to model excitations on perfect or disordered lattices.

Tight-binding models provide analytical expression for the scattering matrices at molecular vertices in the whole exciton band, which allows for immediate analytic continuation to complex values of the quasimomentum/energy, thus enabling description of possible bound exciton states, localized in the vicinity of the scattering center. Therefore, by knowing the exciton scattering properties within an exciton band, one can predict the existence and positions of the bound states with energies being outside of the band, by associating the bound states with the zeros of the analytic continuation of $\det \Gamma(k)$.

Since the presented approach allows the electronic excitations to be characterized using a relatively small number of parameters, i.e., the on-site energies and hopping constants, tight-binding models can and should be used to parameterize the effects of geometric distortions, which leads to efficient description of static disorder, as well as coupling between the electronic and vibrational motions (exciton-phonon coupling). The dependence of the tight-binding parameters on the molecule geometry that fully describes the exciton-phonon Hamiltonian can be obtained in the future by starting with localized distortions, viewing the latter as scattering centers and retrieving the corresponding scattering matrices as a function of distortion, followed by obtaining the dependence of the tight-binding parameters on the value of distortion. This will eventually lead to description of incoherent photoinduced processes in conjugated molecules in terms of the Frenkel-exciton types of Hamiltonians, allowing extension of methods developed in the context of Frenkel exciton systems to much more complicated conjugated structures. In turns, mapping of the band structure obtained from the lattice model into a localized orthogonal basis will allow representation in terms of Wannier functions, a common description used for characterization of delocalized electronic states in semiconductor systems.[37]

ACKNOWLEDGMENTS

This material is based upon work supported by the National Science Foundation under Grant No. CHE-1111350. Los Alamos National Laboratory is operated by Los Alamos National Security, LLC, for the National Nuclear Security Administration of the U.S. Department of Energy under Contract No. DE-AC52-06NA25396. We acknowledge support of Center for Integrated Nanotechnology (CINT) and Center for Nonlinear Studies (CNLS).

[1] S. R. Forrest, Nature (London) **428**, 911 (2004).
[2] W. U. Huynh, J. J. Dittmer, and A. P. Alivisatos, Science **295**, 2425 (2002).
[3] Z. H. Peng, J. S. Melinger, and V. Kleiman, Photosynth. Res. **87**, 115 (2006).
[4] R. Kopelman, M. Shortreed, Z. Y. Shi, W. H. Tan, Z. F. Xu, J. S. Moore, A. Bar-Haim, and J. Klafter, Phys. Rev. Lett. **78**, 1239 (1997).
[5] C. Devadoss, P. Bharathi, and J. S. Moore, J. Am. Chem. Soc. **118**, 9635 (1996).
[6] T. G. Goodson, Acc. Chem. Res. **38**, 99 (2005).
[7] P. F. Barbara, A. J. Gesquiere, S. J. Park, and Y. J. Lee, Acc. Chem. Res. **38**, 602 (2005).
[8] A. J. Heeger, Rev. Mod. Phys. **73**, 681 (2001).
[9] A. J. Heeger, S. Kivelson, J. R. Schrieffer, and W. P. Su, Rev. Mod. Phys. **60**, 781 (1988).
[10] R. H. Friend, R. W. Gymer, A. B. Holmes, J. H. Burroughes, R. N. Marks, C. Taliani, D. D. C. Bradley, D. A. dos Santos, J. L. Brédas, M. Logdlund, and W. R. Salaneck, Nature (London) **397**, 121 (1999).
[11] F. Schindler, J. M. Lupton, J. Muller, J. Feldmann, and U. Scherf, Nature Mater. **5**, 141 (2006).
[12] S. Gunes, H. Neugebauer, and N. Sariciftci, Chem. Rev. **107**, 1324 (2007).
[13] A. Murphy and J. Frechet, Chem. Rev. **107**, 1066 (2007).
[14] H. Sirringhaus, T. Kawase, R. H. Friend, T. Shimoda, M. Inbasekaran, W. Wu, and E. P. Woo, Science **290**, 2123 (2000).
[15] A. J. Heeger, D. J. Heeger, J. Langan, and Y. Yang, Science **270**, 1642 (1995).
[16] E. Menard, M. Meitl, Y. Sun, J.-U. Park, D.-L. Shir, Y.-S. Nam, S. Jeon, and J. Rogers, Chem. Rev. **107**, 1117 (2007).
[17] U. H. F. Bunz, Adv. Polym. Sci. **177**, 1 (2005).
[18] W. Zhang and J. S. Moore, Angew. Chem., Int. Ed. **45**(27), 4416 (2006).
[19] C. J. Cramer, *Computational Chemistry* (John Wiley and Sons Ltd., Chichester, 2004).
[20] C. Wu, S. V. Malinin, S. Tretiak, and V. Y. Chernyak, Nat. Phys. **2**, 631 (2006).
[21] C. Wu, S. V. Malinin, S. Tretiak, and V. Y. Chernyak, Phys. Rev. Lett. **100**, 057405 (2008).
[22] H. Li, C. Wu, S. V. Malinin, S. Tretiak, and V. Y. Chernyak, "Exciton scattering approach for spectroscopic calculations of branched conjugated oligomers," Acc. Chem. Res. (submitted).
[23] C. Wu, S. V. Malinin, S. Tretiak, and V. Y. Chernyak, J. Chem. Phys. **129**, 174111 (2008).
[24] C. Wu, S. V. Malinin, S. Tretiak, and V. Y. Chernyak, J. Chem. Phys. **129**, 174112 (2008).
[25] C. Wu, S. V. Malinin, S. Tretiak, and V. Y. Chernyak, J. Chem. Phys. **129**, 174113 (2008).
[26] H. Li, S. V. Malinin, S. Tretiak, and V. Y. Chernyak, J. Chem. Phys. **132**, 124103 (2010).
[27] H. Li, C. Wu, S. V. Malinin, S. Tretiak, and V. Y. Chernyak, J. Phys. Chem. Lett. **1**, 3396 (2010).
[28] H. Li, C. Wu, S. V. Malinin, S. Tretiak, and V. Y. Chernyak, J. Phys. Chem. B **115**, 5465 (2011).
[29] H. Li, V. Y. Chernyak, and S. Tretiak, J. Phys. Chem. Lett. **3**, 3734 (2012).
[30] M. J. Catanzaro, T. Shi, S. Tretiak, and V. Y. Chernyak, "Topological properties of scattering on graphs: Counting the number of standing waves in quasi-one-dimensional systems" (unpublished).
[31] S. Mukamel, S. Tretiak, T. Wagersreiter, and V. Chernyak, Science **277**, 781 (1997).
[32] S. Tretiak and S. Mukamel, Chem. Rev. **102**, 3171 (2002).
[33] S. Tretiak, A. Saxena, R. L. Martin, and A. R. Bishop, Phys. Rev. Lett. **89**, 097402 (2002).
[34] S. Tretiak, V. Chernyak, and S. Mukamel, J. Phys. Chem. B **102**, 3310 (1998).
[35] T. Minami, S. Tretiak, V. Chernyak, and S. Mukamel, J. Lumin. **87-89**, 115 (2000).
[36] H. Fidder, J. Knoester, and D. A. Wiersma, J. Chem. Phys. **95**, 7880 (1991).
[37] G. H. Wannier, Rev. Mod. Phys. **34**, 645 (1962).
[38] Formally, for a dispersion law, given by Eq. (14), there are two more pairs of "waves" that exist for given frequency ω. A simple analysis shows that they have imaginary wave vectors $\pm i\kappa_1(\omega)$ and $\pm i\kappa_2(\omega)$ with $\kappa_{1,2}(\omega) \sim \ln|J_1/J_2|, \ln|J_1/J_3|$.

This article is copyrighted as indicated in the article. Reuse of AIP content is subject to the terms at: http://scitation.aip.org/termsconditions. Downloaded to IP: 192.12.184.6 On: Mon, 25 Aug 2014 22:50:00